



A Note on Two-Fluid Starting Flow in a Porous Spaced Channel with a Magnetic Field

Komal Goyal^{1,*}, Suripeddi Srinivas¹

¹ Department of Mathematics, School of Advanced Sciences, VIT-AP University, Inavolu-522237, Near Vijayawada, Andhra Pradesh, India

ARTICLE INFO

Article history:

Received 13 March 2023

Received in revised form 12 April 2023

Accepted 10 May 2023

Available online 1 September 2023

Keywords:

Starting flow; Immiscible fluids; Porous space; Eigenfunctions; Hartmann number

ABSTRACT

This study is concerned with starting flow of immiscible fluids in porous space owing to a sudden pressure gradient in the presence of a transverse magnetic field. The flow is divided into two regions, Region1(upper layer) and Region2(lower layer), and they are of variable widths. The required eigenvalues and eigenfunctions, along with the orthogonality, are developed. The analytic solution took on an infinite series structure due to the time-dependent initial transient component of the velocity. Analytical expressions for fluid velocity, volumetric flow rate, and shear stress are evaluated for pertinent parameters. We take cases when channels are filled with air over water and oil over water for analyzing the results. Channel with air over water illustrates that the upper layer is filled with air and the lower layer is filled with water. Similarly, a channel with oil over water illustrates that the upper layer is filled with oil, and the lower layer is filled with water. The effect of Hartmann number and time on velocity profiles has been seen in this study for variable fluid widths in both cases. It is observed that the starting flow velocity slows down with the increase of Hartmann number and porous medium parameter. The effect of the Hartmann number and porous medium parameter on the volumetric flow rate for oil over water case is also shown graphically. For a better understanding of the physical characteristics, the results of shear stress on the lower and upper walls of the channel also have been presented in tabular form.

1. Introduction

Solvent extraction, concentration recovery, chemical reactors, purification of organophilic solutes (such as amino acids and vitamins), and fluid transportation all need knowledge of incompressible immiscible viscous fluids. Due to the vast spectrum of applications of immiscible fluids coupled with starting flow, some interesting studies have been reported in the literature related to starting flow in different geometrical regions [1-6]. When a constant pressure gradient is introduced suddenly, such as when a valve is turned on, this is called starting flow. Perhaps, Wang [5] was the first author to investigate the two-layered starting flow in a channel. Both constant and transient sections of velocity in starting flow can be examined with the help of his research, which is particularly beneficial when suddenly turning on or off the pressure gradient. The flow of incompressible immiscible fluid

* Corresponding author.

E-mail address: komalgoelresearch@gmail.com (Komal Goyal)

<https://doi.org/10.37934/cfdl.15.9.136151>

between two plates with a non-uniform fluid length, i.e., immiscible liquid layers of unequal height, was developed by Kapur and Shukla [7]. With both porous and nonporous tubes, Chamkha [8] explained the flow of two immiscible fluids. Their research is expected to help understand the impact of slag layers on liquid flow and thermal characteristics of coal-fired MHD generators for the case of non-porous tubes. For a diverse channel shape, Erdogan and Imrak [9] studied the exact solution to the time-dependent Navier-Stokes equation when abrupt constant pressure is applied or by impulsive motion in the boundary. Later, Wang [2] explored the transient starting flow of circular, rectangular, and parallel plate geometries in ducts filled with a Darcy- Brinkman medium. Wang [3] presented the unsteady flow in a circular sector duct using the series sum of Bessel integrals. In the presence of the Darcy-Brinkman medium, Wang [6] scrutinized starting flow in a sector duct using the method of Eigenfunction superposition. In a separate investigation, two fluid oscillatory flow in a coated channel is scrutinized by Wang [10], who concluded that Navier's condition does not hold for unsteady core fluids. Starting flow due to an impulsive pressure gradient in a rotating parallel plate channel is investigated by Wang [11], and it is reported that backflow and inertial oscillations occur for higher rates of rotation.

The study of non-Newtonian fluid flow is a captivating research topic in modern times because they exhibit different behaviour than Newtonian fluids. Since Newtonian fluids exhibit a linear stress-strain relationship, non-Newtonian fluids showcase varying viscosities that react in distinct ways to stressors, making their flow characteristics an intriguing concept to analyze. However, it poses challenges to understanding their flow mechanisms in mathematics, physics, and engineering; but because of its widespread applications across various industries, it makes them a crucial area of research. These fluids are categorized as shear-thickening and shear-thinning liquids and have different attributes, including Bingham fluid, viscoelastic fluid, Jeffery fluid, second-grade fluid, and many others. After studying the effect of starting flow on Newtonian fluids, it is essential to investigate the impact of starting flow on non-Newtonian fluids as well, as the behaviour of both fluids is distinct. Khan *et al.*, [12] described the exact solutions of MHD second-grade fluid filled in a porous medium. Their study developed analytic expressions of starting flow for the cases such as flow (a) due to an oscillatory edge, (b) in a duct of a rectangular cross-section oscillating parallel to its length, and (c) due to an oscillatory pressure gradient. Hayat *et al.*, [13] presented an analytic solution employing HAM for a magnetohydrodynamics flow of a second-grade fluid filled in a porous channel. Sharma *et al.*, [14] investigated blood flow in narrow arteries using a two-fluid model, where a non-Newtonian Jeffery fluid filled the core region, and a Newtonian plasma fluid filled the peripheral area. Their study focused on exploring two-fluid flow in a narrow tube with mild stenosis. The results of their research revealed that the velocity decreases with an increase in stenosis height in both the core and peripheral regions. Ewis [15] investigated the influence of Hall current on modified Bingham fluid flow through the parallel plate horizontal channel in the presence of Forchheimer porous medium using the linearized differential transform method (LDTM). Furthermore, based on Ewis [15] and Ewis [16], the author investigated the impact of variable thermal conductivity instead of constant thermophysical properties on the flow of viscoelastic fluid in a vertical channel. This research aimed to improve our understanding of the influence of non-linear radiation and dissipation on the flow characteristics of viscoelastic fluids. Motivated by Sharma *et al.*, [14], Sharma and Yadav [17] presented a mathematical model to investigate the impact of a magnetic field on blood flow through narrow tubes in stenosis. Their study scrutinized the effect of Hartmann number, shape, and size of the stenosis on the velocity, volumetric flow rate, and wall shear stress. As creeping flow is relevant in many biological systems, in their study, Khanukaeva *et al.*, [18] investigated the behaviour of micropolar fluid flow through the swarm of cylindrical cells with a porous layer using numerical simulations, aiming to deepen our understanding of this complex

phenomenon and its applications. In the presence of a porous medium, Yadav [19] explored the behaviour of porous cylindrical shells in the concentric cylindrical cavity.

As the study of magnetic field effects on fluid flow has significant implications for understanding the fundamental physics of fluid dynamics and the development of novel technologies. Yadegari and Jahangiri [20] investigated the effect of a non-uniform magnetic field, i.e., a magnetic field with different intensities, on blood flow using the COSMOL Finite Element Software. Their study was motivated by the importance and necessity of biomedicines in engineering studies. In the presence of a transverse magnetic field and a constant pressure gradient, the two-layered flow of immiscible, electrically conducting incompressible viscous fluids of varied viscosity in a channel filled with porous media in two separate layers of equal width has been explored by Ansari and Deo [21]. Srinivas *et al.*, [22] investigated the hydromagnetic characteristics of Casson fluid pulsatile flow in a vertical porous channel, by examining the impact of thermal radiation and chemical reaction. Recently, Bhat *et al.*, [23] conducted a study on the heat and mass transfer analysis of micropolar fluid flow between porous walls in the presence of a magnetic field. Their research focused on analyzing the flow characteristics by considering different permeability of the porous medium. The influence of hall current, thermal radiation, heat source, and chemical reaction on the heat and mass transfer characteristics of a two-layered immiscible fluid flowing through a vertical channel was investigated by Devi and Srinivas [24]. In a recent investigation pertaining to starting flows, Wang [5] studied the starting flow in a channel filled with two immiscible fluids and observed that normalized slip length is not constant for starting flows.

As far as the authors know, relatively scant attention has been given by the researchers to starting flow under the influence of a magnetic field, with unequal fluid width layers in layered immiscible flows. Keeping that in mind, the problem is modelled in such a way that the width of the layers can be varied. As such, a study has yet to be explored. Hence the main objective of this work is to investigate the effect of fluid width parameters on the flow field for sundry pertinent parameters theoretically. It is fascinating to see how this study clarifies what occurs when (i) upper fluid dominates the fluid flow and (ii) both fluids dominate the fluid flow equally. One of the essential applications of this study is when we abruptly turn on or off the fluid flow. To extend the applicability of this model to other fields, we introduce a porous medium into the horizontal channel. This enhancement enables the model to be applied in geothermal, geophysical engineering, and petroleum sediment retrieval. Hence this research is to study the starting flow in porous space with a magnetic field when both immiscible fluids travel with different velocities in the presence of a sudden pressure gradient. Transient solutions are derived in the form of eigenfunction expansions, where the eigenvalues are determined by solving the characteristic equations numerically. The classical no-slip condition at the boundary and matching conditions at the interface of both mediums are used. The effect of Hartmann number and other emerging parameters on velocity distribution and mass flux are depicted graphically using Mathematica software and discussed in detail.

Further, the paper is organised as follows. The mathematical formulation of the problem is presented in Section 2. Section 3 comprises the transient solution to the problem. All the non-dimensional quantities (shear stress and volumetric flow rate) are presented in section 4. With the aid of graphs, results and discussions is made in Section 5. Finally, the main findings are listed in Section 6.

2. Formulation of the Problem

Consider fully developed two layers of immiscible, incompressible, viscous fluids with different densities and viscosities flowing over a porous space of length l (see Figure 1). The upper and lower

layers of fluid are denoted by region-1 and region-2, respectively. In the channel, region-1 is occupied by lighter fluid, which is between $\epsilon l < y' \leq l$ where $0 < \epsilon < 1$, and region-2 is occupied by the heavier fluid, which is between $0 \leq y' < \epsilon l$. The permeability of the porous medium is assumed to be the same in both layers. Both the walls of the channel are at rest, and the flow is subjected to a sudden constant pressure gradient $\partial p / \partial x'$. Moreover, the influence of a transverse magnetic field of uniform intensity is set at a right angle to the direction in which the fluid moves.

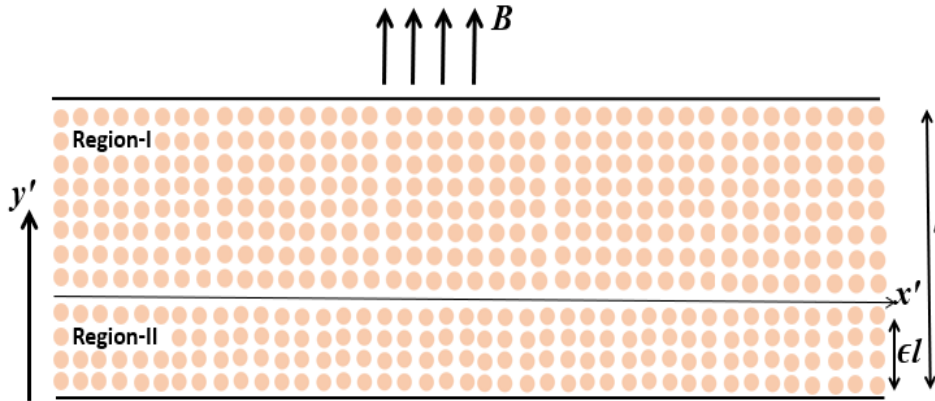


Fig. 1. Flow configuration of the model

To simplify the governing equations, the following assumptions are considered (see Mahmoudi [25], Yang and Vafai [26], and Boutin *et al.*, [27]).

- i. In the porous medium, the flow is laminar and incompressible.
- ii. The porous medium is isotropic and homogenous in both regions.
- iii. The fluid and solid phases in the porous medium are assumed to have constant thermophysical properties.
- iv. Flow is considered two-dimensional, and channel walls are impermeable.

Based on the aforementioned assumptions, the corresponding flow equation reduces to (see Wang [5], Ansari and Deo [21], and Umavathi *et al.*, [28]),

$$\rho_1 u'_{1t'} = -\frac{\partial p}{\partial x'} + \mu_1 u'_{1y'y'} - \frac{\mu_1 u'_1}{k} - \sigma_1 B_o^2 u'_1 \tag{1}$$

$$\rho_2 u'_{2t'} = -\frac{\partial p}{\partial x'} + \mu_2 u'_{2y'y'} - \frac{\mu_2 u'_2}{k} - \sigma_2 B_o^2 u'_2 \tag{2}$$

Here k , ρ , u' , t' , and p represents the permeability of the porous medium, density, dimensional velocity, time and pressure respectively. The magnetic induction vector of the uniform magnetic field applied is represented by B , σ is the electric conductivity and μ is the dynamic viscosity. Where $B_0 = |B|$. The numerical subscripts indicate the region that is being considered. The pressure gradient that is applied is

$$-\frac{\partial p}{\partial x'} = g \cdot H(t') \tag{3}$$

Here, g is the constant magnitude of the pressure gradient, and the unit step function is represented as H . Normalize time by $l^2 \rho_1 / \mu_1$, length by l , and velocity by gl^2 / μ_1 . Eq. (1) and Eq. (2), on dropping the primes, becomes:

$$u_{1t} = H(t) + \mu_1 \frac{\partial^2 u_1}{\partial y^2} - (n^2 + M_1^2) u_1 \quad (4)$$

$$u_{2t} = \beta^2 H(t) + \left(\frac{\beta}{\alpha}\right)^2 \frac{\partial^2 u_2}{\partial y^2} - (n^2 + M_2^2) \left(\frac{\beta}{\alpha}\right)^2 u_2 \quad (5)$$

addressing the following dimensionless ratios are

$$\alpha^2 = \frac{\mu_1}{\mu_2}, \quad \beta^2 = \frac{\rho_1}{\rho_2}, \quad \gamma^2 = \frac{\sigma_1}{\sigma_2} \quad (6)$$

The fluid flow through the porous medium was analyzed using Darcy's law for viscous fluid in the governing Eq. (4) and Eq. (5). The porous medium parameter was used to characterize the effect, which defines the correlation between the characteristic length and permeability of porous medium (see Ananth *et al.*, [29]). Moreover, the Hartmann number is a measure of the ratio of electromagnetic force to viscous force. So, correspondingly here, M_1 and M_2 represent the Hartmann numbers of region-I and region-II, respectively.

Since velocity on both the walls becomes zero, the boundary conditions are:

$$u_1(1, t) = 0 \quad (7)$$

$$u_2(0, t) = 0 \quad (8)$$

and thus, at the interface, the velocities and stresses match (see Ansari and Deo [21], and Wang [5])

$$u_1(\varepsilon, t) = u_2(\varepsilon, t) \quad (9)$$

$$\alpha^2 u_{1y}(\varepsilon, t) = u_{2y}(\varepsilon, t) \quad (10)$$

For the starting flow problem, an over-bar denotes a steady-state solution, whereas a tilde denotes a transient solution.

$$u_i(y, t) = \bar{u}_i(y) - \tilde{u}_i(y, t), \quad i = 1, 2 \quad (11)$$

Then, Eq. (4) and Eq. (5) give,

$$\bar{u}_{1yy} - (n^2 + M_1^2) \bar{u}_1 = -1, \quad (12a)$$

$$\bar{u}_{2,yy} - (n^2 + M_2^2)\bar{u}_2 = -\alpha^2 \quad (12b)$$

$$\tilde{u}_{1,yy} - (n^2 + M_1^2)\tilde{u}_1 = \frac{\partial \tilde{u}_1}{\partial t}, \quad (13a)$$

$$\tilde{u}_{2,yy} - (n^2 + M_2^2)\tilde{u}_2 = \frac{\partial \tilde{u}_2}{\partial t} \left(\frac{\alpha}{\beta} \right)^2 \quad (13b)$$

Eq. (7) to Eq. (8) are likewise satisfied by the steady and transient velocities. Furthermore, velocity is considered to be zero in the beginning, i.e.

$$\tilde{u}_i(y, 0) = \bar{u}_i(y), \quad i=1,2 \quad (14)$$

On solving Eq. (12a) and Eq. (12b) subjected to the condition in Eq. (7) to Eq. (10), the solution is:

$$\bar{u}_1(y) = B_1 \left[e^{-\sqrt{n^2+M_1^2}y} - e^{\sqrt{n^2+M_1^2}(y-2)} \right] + \frac{1}{n^2 + M_1^2} \left[1 - e^{\sqrt{n^2+M_1^2}(y-1)} \right] \quad (15)$$

$$\bar{u}_2(y) = -2B_2 \sinh(\sqrt{n^2 + M_2^2} y) + \frac{\alpha^2}{n^2 + M_2^2} \left[1 - e^{\sqrt{n^2+M_2^2}y} \right] \quad (16)$$

B_1, B_2 and other coefficients are given below is the precise steady-state solution.

$$k_1 = \sqrt{n^2 + M_1^2}, \quad k_2 = \sqrt{n^2 + M_2^2}, \quad a^2 = (k_1 \alpha / \beta)^2 - k_2^2, \quad n = l / \sqrt{k}, \quad M_1 = \sqrt{\sigma_1 B_o^2 L^2 / \mu_1},$$

$$M_2 = M_1 (\alpha / \gamma)^2, \quad A_n = D_n / C_n, \quad D_n = \int_0^1 W \bar{U} \Phi_n dy, \quad a_n = \sin \left[\sqrt{\lambda_n^2 - k_1^2} (1 - \varepsilon) \right] / \sin \left[\sqrt{\left(\frac{\lambda_n \alpha}{\beta} \right)^2 - k_2^2} \varepsilon \right]$$

$$B_1 = e^{k_1 \varepsilon} \left[B_2 \left\{ \frac{k_2 \cosh(k_2 \varepsilon)}{k_1 \alpha^2} - \sinh(k_2 \varepsilon) \right\} + \frac{1}{2} \left\{ \frac{\alpha^2}{k_2^2} - \frac{1}{k_1^2} \right\} + \frac{e^{k_2 \varepsilon}}{2k_2^2} \left\{ \frac{k_2}{k_1} - \alpha^2 \right\} \right],$$

$$B_2 = \frac{1}{2 \sinh(k_2 \varepsilon)} \left[B_1 \left\{ e^{k_1(\varepsilon-2)} - e^{-k_1 \varepsilon} \right\} + \frac{1}{k_1^2} \left\{ e^{(\varepsilon-1)k_1} - 1 \right\} + \frac{\alpha^2}{k_2^2} \left\{ 1 - e^{k_2 \varepsilon} \right\} \right]$$

The case of the transient problem is more complex, and the solution is obtained by eigenfunction expansions.

3. Transient Solution

The series is recommended based on the form of Eq. (13a) and Eq. (13b),

$$\tilde{u}_i(y, t) = \sum_{n=1}^{\infty} A_n \phi_{in}(y) e^{-\lambda_n^2 t}, \quad i=1,2 \quad (17)$$

A_n are the constant coefficients and ϕ_{in} is the eigenfunction to be calculated. Eq. (13a), Eq. (13b) becomes

$$\phi_{1n}''(y) + (\lambda_n^2 - k_1^2)\phi_{1n}(y) = 0 \tag{18}$$

$$\phi_{2n}''(y) + \left\{ \left(\frac{\lambda_n \alpha}{\beta} \right)^2 - k_2^2 \right\} \phi_{2n}(y) = 0 \tag{19}$$

respective boundary conditions are:

$$\phi_{1n}(1) = 0, \quad \phi_{2n}(0) = 0 \tag{20}$$

Eq. (18) to Eq. (20), apart from constant multiple, gives:

$$\phi_{1n}(y) = \sin \left[\sqrt{\lambda_n^2 - k_1^2} (1-y) \right], \tag{21a}$$

$$\phi_{2n}(y) = a_n \sin \left[\sqrt{\left(\frac{\lambda_n \alpha}{\beta} \right)^2 - k_2^2} y \right] \tag{21b}$$

The matching condition gives us the constant a_n and the eigenvalue λ_n .

$$\phi_{1n}(\varepsilon) = \phi_{2n}(\varepsilon) \tag{22}$$

$$\alpha^2 \phi_{1n}'(\varepsilon) = \phi_{2n}'(\varepsilon) \tag{23}$$

Eq. (22) and Eq. (23) also provide the characteristic equation.

$$\alpha^2 \sqrt{\lambda_n^2 - k_1^2} \cos \left[\sqrt{\lambda_n^2 - k_1^2} (1-\varepsilon) \right] \sin \left[\sqrt{\left(\frac{\lambda_n \alpha}{\beta} \right)^2 - k_2^2} \varepsilon \right] + \sqrt{\left(\frac{\lambda_n \alpha}{\beta} \right)^2 - k_2^2} \cos \left[\sqrt{\left(\frac{\lambda_n \alpha}{\beta} \right)^2 - k_2^2} \varepsilon \right] \tag{24}$$

$$\sin \left[\sqrt{\lambda_n^2 - k_1^2} (1-\varepsilon) \right] = 0$$

Thus, for given α^2 , k_1^2 , k_2^2 and ε , the sequence of eigenvalues λ_n can be numerically investigated.

The composite eigenfunction is represented by each eigenvalue.

$$\Phi_n = \begin{cases} \phi_{1n}(y), & \varepsilon < y \leq 1 \\ \phi_{2n}(y), & 0 \leq y < \varepsilon \end{cases} \tag{25}$$

We set $n \neq m$ to demonstrate the orthogonality property,

$$\int_0^1 w \Phi_n \Phi_m dy = 0 \tag{26}$$

w represents the weighting function for composite regions. Using considerable investigation and the application of a_n , we have discovered.

$$w = \begin{cases} \beta^2, & \varepsilon < y \leq 1 \\ 1, & 0 \leq y < \varepsilon \end{cases} \tag{27}$$

The integral is positive definite for $n = m$,

$$C_n = \int_0^1 W \Phi_n^2 dy \tag{28}$$

Consider the velocities for their respective composite regions to be defined respectively,

$$\tilde{u} = \begin{cases} \tilde{u}_1 \\ \tilde{u}_2 \end{cases}, \quad \bar{u} = \begin{cases} \bar{u}_1 \\ \bar{u}_2 \end{cases}, \quad u = \begin{cases} u_1 \\ u_2 \end{cases} \tag{29}$$

Eq. (17) reduces to:

$$\tilde{u} = \sum_{n=1}^{\infty} A_n \Phi_n e^{-\lambda_n^2 t} \tag{30}$$

Eq. (14) gives:

$$\bar{u} = \sum_{n=1}^{\infty} A_n \Phi_n \tag{31}$$

A_n and D_n are the coefficients obtained by multiplying Eq. (31) by $w \Phi_m$ and integrating from 0 to 1.

4. Non-Dimensional Quantities

4.1 Mass Flux

The instantaneous flow rate is calculated using

$$Q(t) = \int_0^1 u dy \tag{32}$$

here starting velocity is:

$$u = \bar{u} - \tilde{u} \tag{33}$$

4.2 Shear Stress

Non-dimensional shear stress for respective walls is given by [24]:

$$\tau_1 = \frac{\partial u_1}{\partial y} \Big|_{y=1}, \quad \tau_2 = \frac{1}{\alpha^2} \frac{\partial u_2}{\partial y} \Big|_{y=0} \tag{34}$$

Here, $y=0$ indicates the lower boundary, and $y=1$ indicates the upper boundary.

5. Results and Discussions

For varying channel widths, we examine two frequent instances, case-I as air over water and case-II as oil over water. From now onwards, we will use it in our entire manuscript. To begin, consider case-I in a channel with a density ratio $\rho_1/\rho_2 = 0.0012$ and a viscosity ratio $\mu_1/\mu_2 = 0.018$ while maintaining an electric conductivity ratio $\sigma_1/\sigma_2 = 0.5$. As a result, we get $\alpha = 0.134$, $\beta = 0.035$, and $\gamma^2 = 0.5$.

Starting fluid flow is more complicated to handle than steady-state flow because of the presence of the transient section, where the velocity of the fluid changes over time. The numerical root-finding approach is adopted to determine the eigenvalues from Eq. (24). Eq. (17), Eq. (29), and Eq. (33) and A_n is used to calculate fluid velocity. The physical values used for the computations are provided in Table 1. Table 2 shows the eigenvalues in the absence of a transverse magnetic field ($M_1 = 0$) for varied channel widths $\varepsilon=0.1$ and 0.5 in base-I and case-II with $n=2$ and $n=0.1$, respectively.

Similarly, in both situations for different channel widths $\varepsilon = 0.1$ and 0.5 , using Eq. (24), Table 3 and Table 4 illustrate the eigenvalues for the constant time $t=1$, and porous medium parameter $n=2$ for varied Hartmann numbers. From Figure 2, water being of greater viscosity occupies a smaller width in the channel, and air dominates the fluid flow. One can observe from Figure 2(a) that for the fluid in region-2, the velocity profiles are flat, and for region-1, the profiles are parabolic in nature. For oil over the water case, velocity is more like flat initially and enhanced with a rise in t .

Table 1
 Physical values, at room temperature, for air, water, and corn oil [13]

Fluid	Density (Kg/m^3)	Viscosity (Pa.s)
Air	1.2-1.3	0.000018
Water	1000	0.001
Corn oil	911	0.016-0.034

Table 2
 Eigenvalues for velocity profile keeping same Hartmann number $M_1 = 0$, varying time in a channel

ε	Air over Water	Oil over Water
0.1	3.4073	1.8960
0.5	0.8110	2.4410

Table 3
 Eigenvalues for velocity profile keeping time constant $t = 1$, and porous medium parameter $n=2$, varying Hartmann number in a channel for air over water

ε	$M_1=1$	$M_1=1.5$	$M_1=2$	$M_1=2.5$
0.1	3.3372	3.1924	2.9321	2.5354
0.5	1.0952	3.2358	2.9541	2.5465

Table 4
 Eigenvalues for velocity profile keeping time constant $t = 1$, and porous medium parameter $n=2$, varying Hartmann number in a channel for oil over water

ε	$M_1=1$	$M_1=1.5$	$M_1=2$	$M_1=2.5$
0.1	1.9096	1.9259	1.9478	1.9745
0.5	1.7635	1.9201	2.1166	2.3387

From Figure 2(a) and Figure 3(a), by analysis of the results in both cases, it can be observed that the location of the maximum velocity differs depending on whether air or oil dominates the fluid flow

in a channel filled with air-water or oil-water, respectively. For the former, the maximum velocity is found in the upper region of the channel, while for the latter case, it occurs at the fluid flow interface. Moreover, the increase in the maximum velocity value from $t=0.01$ to steady state is 64.79% in case-I, which is lower than the corresponding increase of 97.113% in case-II.

Figure 2(b) and Figure 3(b) reveal that with the rise in the magnetic field velocity of the fluid reduces. As in the presence of an applied magnetic field, there is a drag force in the opposite direction of the flow field, leading to a fall in velocity distribution with the strength of the magnetic field.

For the equal fluid width layers, we have presented velocity distributions in Figure 4 and Figure 5 for case-I and case-II, respectively. In the absence of a magnetic field, velocity achieves a steady state relatively quickly over shorter periods of time. It hence causes overlapping profiles for the porous channel (see Figure 4(a) and Figure 5(a)). Furthermore, Figure 4(a) delineates that since both fluids dominate the fluid flow equally, the flow is driven by the difference in pressure between the two fluids. Since air is less dense than water, it offers less resistance to the flow than water. This means that the pressure drop across the air-filled region is lower than that across the water-filled region. As a result, the fluid velocity in the air-filled region is higher than in the water-filled region. Additionally, viscosity is also a measure of a fluid's resistance to flow. Corn oil has a higher viscosity than water, which means it offers more resistance to flow than water. And, due to its higher viscosity, the pressure drops across the region filled with corn oil is higher than that across the region filled with water. As a result, the fluid velocity in the corn oil-filled region is lower than in the water-filled region. This means that the maximum velocity will occur in the region filled with water, where the fluid encounters less resistance to flow, as depicted in Figure 5(a). Figure 4(b) and Figure 5(b) demonstrate that an increasing Hartmann number leads to a reduction in the starting velocity of the liquid flow. This phenomenon occurs due to the generation of retarding forces, which take the form of a conductive drag force and slow down the fluid velocity.

The porous medium parameter refers to the degree of porosity of a material or medium. A highly porous medium contains a large number of small spaces or pores, which can affect the movement of fluids or particles through the material. When the porous medium parameter increases, the medium becomes more resistant to the flow of fluids or particles. This is because the pores in the medium offer more resistance to the movement of the fluid or particles, and the fluid or particles have to travel through more tortuous paths to move through the medium. As a result, the rise in the porous medium parameter dampens the starting velocity, which is evident from Figure 6.

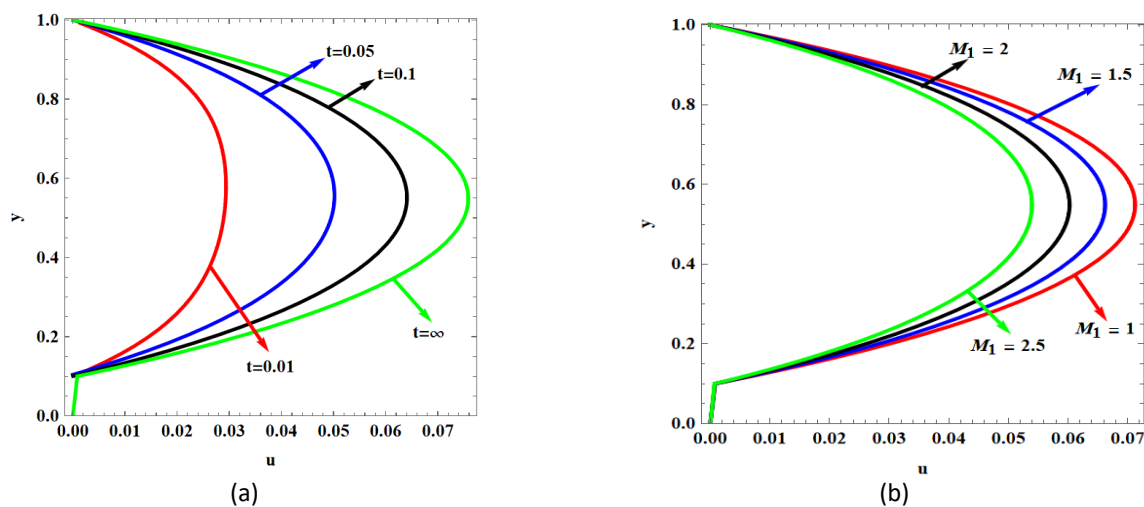


Fig. 2. Velocity distribution for case-I with porous medium parameter $n=2$, $\varepsilon=0.1$ (a) $M_1=0$ from bottom: $t=0.01, 0.05, 0.5, \infty$, (b) $t=1$, from bottom: $M_1=2.5, 2, 1.5, 1$

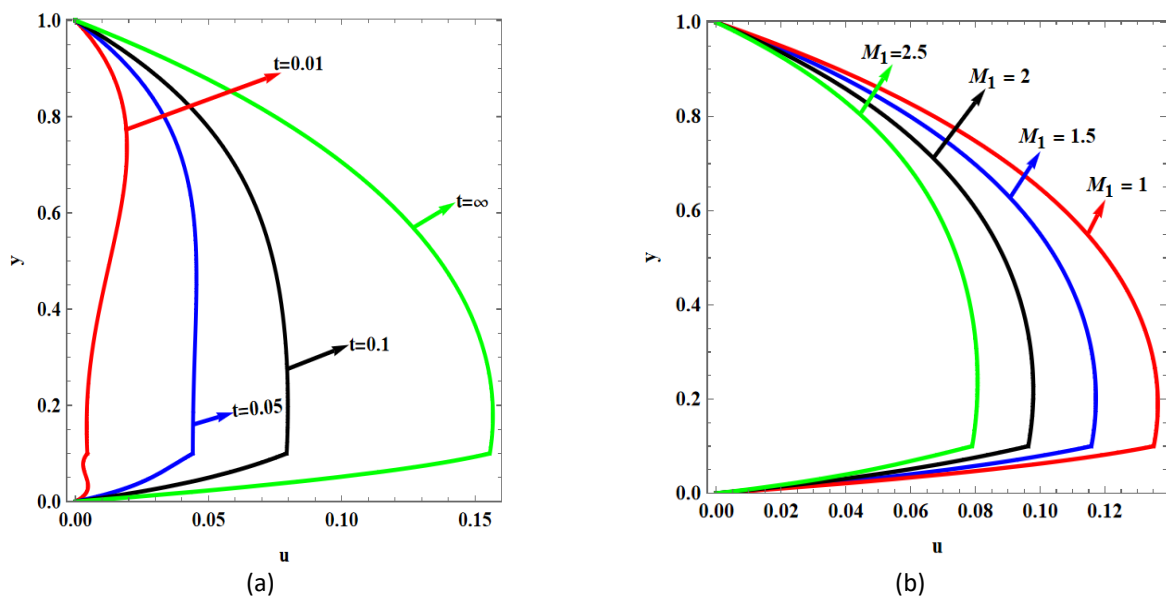


Fig. 3. Velocity distribution for case-II with porous medium parameter $n=2$, $\varepsilon=0.1$ (a) $M_1=0$ from bottom: $t=0.01, 0.05, 0.5, \infty$, (b) $t=1$, from bottom: $M_1= 2.5, 2, 1.5, 1$

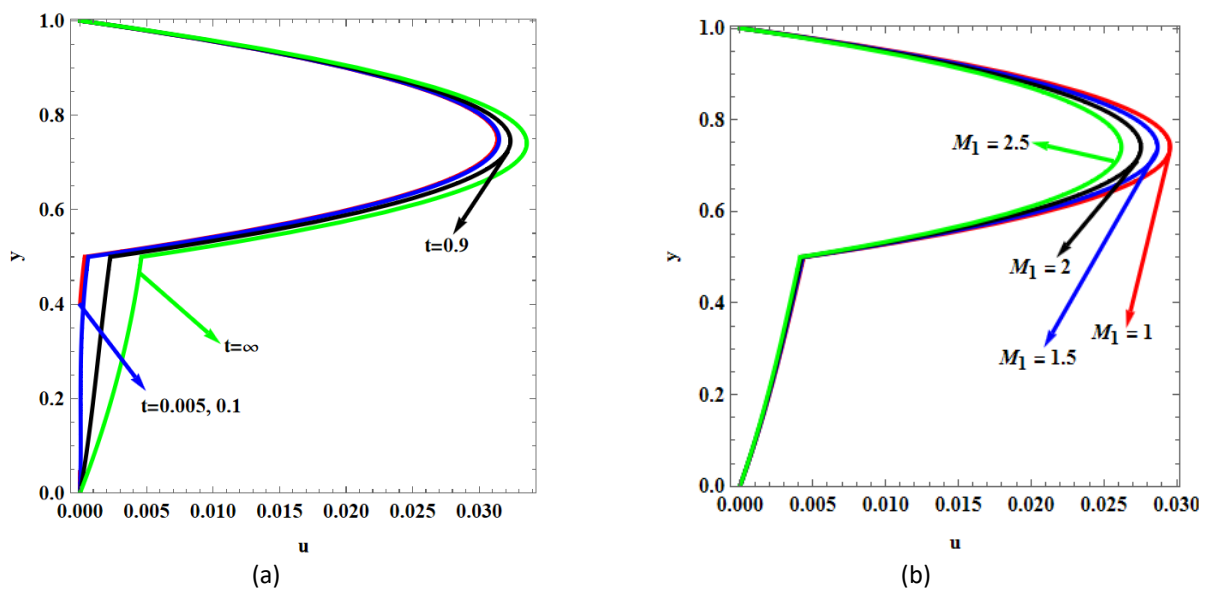


Fig. 4. Velocity distribution for case-I with $\varepsilon=0.5$, (a) $M_1=0$, porous medium parameter $n=0.1$ from bottom: $t=0.005, 0.1, 0.9, \infty$, (b) Porous medium parameter $n=2$, $t=1$ from bottom: $M_1= 2.5, 2, 1.5, 1$

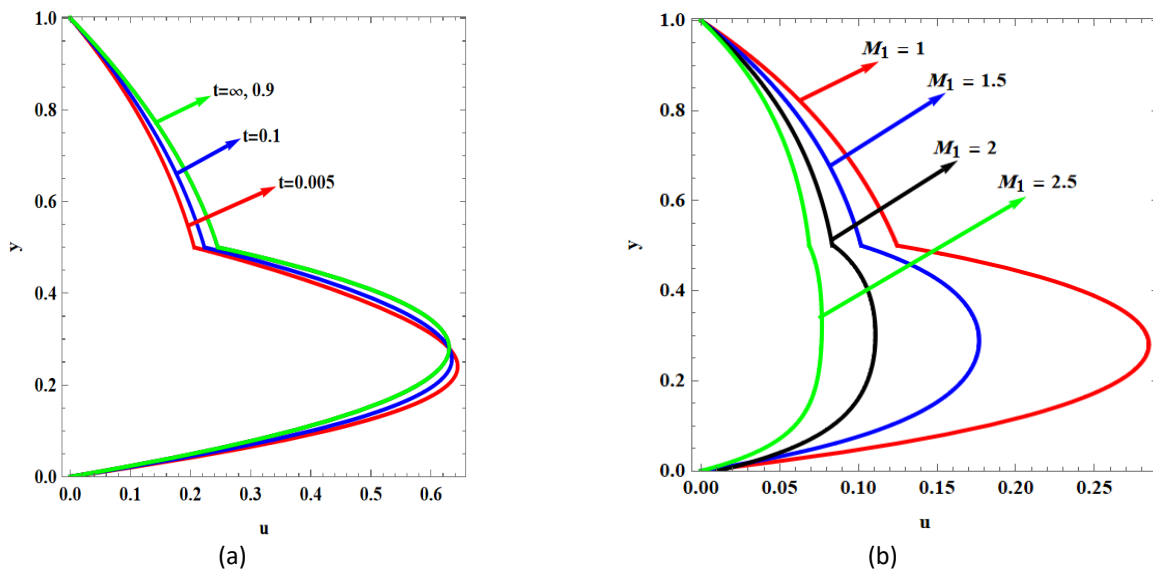


Fig. 5. Velocity distribution for case-II with $\varepsilon = 0.5$ (a) $M_1=0$, porous medium parameter $n=0.1$, from bottom: $t=0.005, 0.1, 0.9, \infty$, (b) Porous medium parameter $n=2$, $t=1$ from bottom: $M_1= 2.5, 2, 1.5, 1$

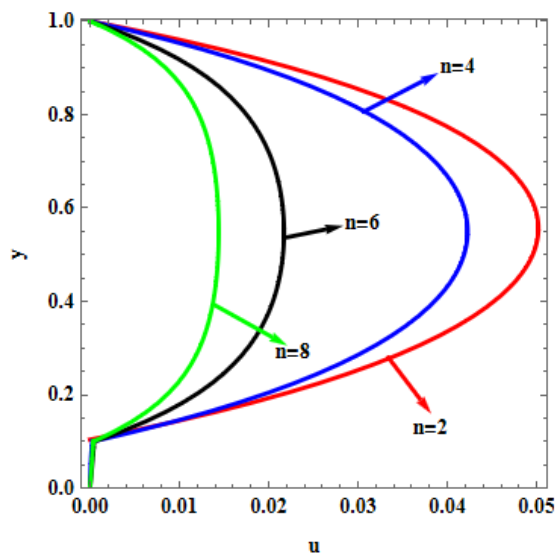


Fig. 6. Velocity distribution for case-I with $M_1=0$, $\varepsilon = 0.1$, $t=0.05$, from bottom: $n=8, 6, 4, 2$

A comparative study is performed in Table 5 for the velocity distribution for the case of air over water with $n=0.1$ and $M_1 = 0$. The results are found to be in good agreement.

Table 5

Comparative study of velocity distribution for the case-I (air over water)

y/u	Hayat <i>et al.</i> , [13]	Present
0	0.0000	0.0000
0.2	0.0424	0.0424
0.4	0.0931	0.0931
0.6	0.1031	0.1031
0.8	0.0723	0.0724
1	0.0019	0.0010

Variations of stress at the lower and upper walls of the channel for different parameters are presented in Table 6. The stress at the upper wall is more significant when compared to the stress at the lower wall, which is evident from the tables. When M_1 is fixed, it is observed that the stress for the case of air over the water is large (see Table 6(a), Table 6(b), Table 6(d), Table 6(e)).

Table 6

Variation of shear stress (a) Air over water for varying time $n=2$, $M_1=1$, (b) Air over water for varying porosity parameter $t=0.02$, $M_1=1$, (c) Air over water for varying Hartmann number $t=0.02$, $n=1$, (d) Oil over water for varying time $n=2$, $M_1=1$, (e) Oil over water for varying porosity parameter $t=0.02$, $M_1=1$, (f) Oil over water for varying Hartmann number $t=0.02$, $n=1$

$t \setminus \epsilon$		0.25	0.5	0.75
0.005	$y=0$	2.2312	1.6910	1.9380
	$y=1$	1.1387	0.3089	0.1665
0.02	$y=0$	1.9502	1.6835	1.9410
	$y=1$	0.8925	0.3163	0.1647
0.1	$y=0$	1.3612	1.6533	1.9522
	$y=1$	0.3764	0.3461	0.1580
1	$y=0$	1.2420	1.6065	1.9656
	$y=1$	0.2721	0.3924	0.1499
∞	$y=0$	1.2420	1.6063	1.9657
	$y=1$	0.2721	0.3926	0.1498

(a)

$t \setminus \epsilon$		0.25	0.5	0.75
0.005	$y=0$	0.0572	0.2033	0.4106
	$y=1$	-7.0600	-2.6258	-0.9968
0.02	$y=0$	0.0644	0.2012	0.4162
	$y=1$	-7.0873	-2.6318	-0.9974
0.1	$y=0$	0.0927	0.1932	0.4362
	$y=1$	-7.1949	-2.6537	-0.9995
1	$y=0$	0.1335	0.1844	0.4556
	$y=1$	-7.3502	-2.6777	-1.0015
∞	$y=0$	0.1336	0.1844	0.4557
	$y=1$	-7.3506	-2.6777	-1.0015

(d)

$n \setminus \epsilon$		0.25	0.5	0.75
2	$y=0$	1.9502	1.6835	1.9410
	$y=1$	0.8925	0.3163	0.1647
2.5	$y=0$	2.1236	1.5731	2.1567
	$y=1$	1.8036	0.7958	0.2709
3	$y=0$	1.5465	1.6272	2.5528
	$y=1$	2.1253	1.2033	0.3490
3.5	$y=0$	1.3194	1.7323	3.1386
	$y=1$	3.1254	1.6652	0.4330
4	$y=0$	1.2038	1.8945	3.9938
	$y=1$	4.6856	2.1938	0.5173

(b)

$n \setminus \epsilon$		0.25	0.5	0.75
2	$y=0$	0.0644	0.2012	0.4162
	$y=1$	-7.0873	-2.6318	-0.9974
2.5	$y=0$	0.0676	0.1297	0.3291
	$y=1$	-9.0573	-2.8613	-0.9834
3	$y=0$	0.0430	-0.0598	0.2038
	$y=1$	-11.1449	-3.0959	-0.9719
3.5	$y=0$	0.0287	-0.1211	0.0025
	$y=1$	-13.7391	-3.4524	-0.9653
4	$y=0$	0.0198	-0.1998	-0.3052
	$y=1$	-17.0806	-3.8660	-0.9536

(e)

$M_1 \setminus \epsilon$		0.25	0.5	0.75
0.5	$y=0$	0.5230	1.6693	1.7496
	$y=1$	-1.2382	-0.2420	-0.1056
1	$y=0$	0.5256	1.7127	1.8325
	$y=1$	-1.2161	-0.2202	-0.0864
1.5	$y=0$	1.7451	1.7688	1.9778
	$y=1$	-0.2008	-0.1999	-0.0566
2	$y=0$	2.0601	1.8356	2.1691
	$y=1$	0.2981	-0.1847	-0.0472
2.5	$y=0$	2.1210	1.8214	2.4402
	$y=1$	0.4526	-0.0795	-0.0415

(c)

$M_1 \setminus \epsilon$		0.25	0.5	0.75
0.5	$y=0$	0.0120	0.2888	0.5898
	$y=1$	-1.6105	-1.6371	-1.1155
1	$y=0$	0.0141	0.1959	0.5162
	$y=1$	-4.2410	-2.6557	-0.9864
1.5	$y=0$	0.0171	0.2485	0.5825
	$y=1$	-6.4970	-3.6595	-1.0430
2	$y=0$	0.0205	0.2296	0.6283
	$y=1$	56.7818	-4.5144	-1.1924
2.5	$y=0$	0.0246	0.2148	0.6831
	$y=1$	902.132	2.8065	-1.3518

(f)

Figure 7(a) depicts the transient increase in the volumetric flow rate. We can observe that for larger n , the steady-state occurs significantly sooner. This is because, for larger n , the time exponent

parameter λ_n is greater. Further, from Figure 7(b), one can observe that the volumetric flow rate (fixed time) decreases with a rise in the strength of the magnetic field.

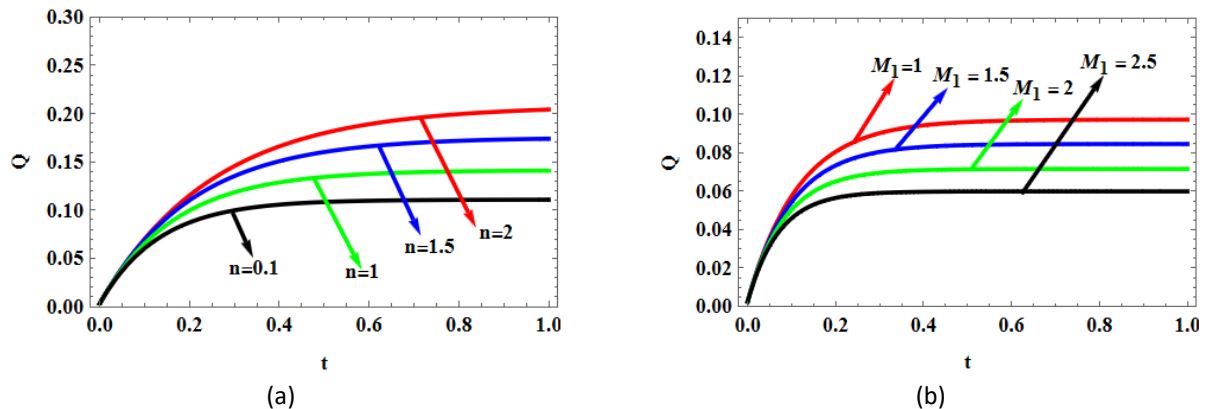


Fig. 7. Volumetric flow rate profiles for oil over water with $\varepsilon=0.1$, (a) $M_1=0$, porous medium parameter $n=0.1, 1, 1.5, 2$, (b) $n=2$, Hartmann number $M_1=1, 1.5, 2, 2.5$

6. Conclusions

The effect of a transverse magnetic field on the flow of two-layered viscous immiscible fluids in porous space was investigated in this note. To maintain the continuity of the flow at the interface, conditions related to the continuity of the velocity and stress are imposed. We developed the required eigenvalues, eigenfunctions, as well as orthogonality. The situation of two cases of physical immiscible fluids with porous medium parameter, channel fluid width, and transverse magnetic field are discussed in this study. This type of studies can be applied to a variety of fields, including chemical engineering, environmental monitoring, biomedical engineering, material processing, and the oil and gas industry. The potential advantages of such applications include the separation of oil and water, the investigation of water flow in rivers and oceans, the design of reactors, the production of plastics and polymers, and much more. Important observations are summarised below:

- i. Larger the porous medium parameter, the sooner will be the occurrence of steady-state in the volumetric flow rate.
- ii. The volumetric flow rate decreases with a rise in the strength of the magnetic field.
- iii. There is larger stress at the upper wall as compared to the lower wall of the channel.
- iv. For case-I (air over water), channel walls experience greater stress when compared to case-II (oil over water) (from Table 6(a), Table 6(d), Table 6(b), and Table 6(e)).
- v. By taking $M_1=0$, the results for the hydrodynamic case for the corresponding problem can be captured. Further, In the absence of a magnetic field and porous space, the results of Wang [5] can be recovered, as a special case, from our analysis.

Hopefully, this analytical study will be useful in assessing the accuracy of numerical solutions to more complicated problems in this direction, accounting greater number of physical parameters. Even though various studies have been reported with pulsatile flow, so far, no analytical work has been reported pertaining to the thermal aspects of immiscible starting flow (with a sudden pressure gradient) from the author's perception, and it is still an open problem.

Acknowledgement

This research was not funded by any grant.

References

- [1] Ng, Chiu-On. "Starting flow in channels with boundary slip." *Meccanica* 52 (2017): 45-67. <https://doi.org/10.1007/s11012-016-0384-4>
- [2] Wang, C. Y. "The starting flow in ducts filled with a Darcy–Brinkman medium." *Transport in porous media* 75 (2008): 55-62. <https://doi.org/10.1007/s11242-008-9210-3>
- [3] Wang, C. Y. "Unsteady flow in a circular sector duct." *International Journal of Non-Linear Mechanics* 46, no. 1 (2011): 291-295. <https://doi.org/10.1016/j.ijnonlinmec.2010.09.010>
- [4] Wang, C. Y. "Starting flow in regular polygonal ducts." *Fluid Dynamics Research* 48, no. 3 (2016): 035505. <https://doi.org/10.1088/0169-5983/48/3/035505>
- [5] Wang, C. Y. "Starting flow in a channel with two immiscible fluids." *Journal of Fluids Engineering* 139, no. 12 (2017). <https://doi.org/10.1115/1.4037495>
- [6] Wang, C. Y. "Starting Darcy–Brinkman Flow in a Sector Duct Using the Method of Eigenfunction Superposition." *Transport in Porous Media* 127 (2019): 631-642. <https://doi.org/10.1007/s11242-018-1217-9>
- [7] Kapur, J. N., and J. B. Shukla. "The flow of incompressible immiscible fluids between two plates." *Applied Scientific Research, Section A* 13 (1964): 55-60. <https://doi.org/10.1007/BF00382036>
- [8] Chamkha, Ali J. "Flow of two-immiscible fluids in porous and nonporous channels." *J. Fluids Eng.* 122, no. 1 (2000): 117-124. <https://doi.org/10.1115/1.483233>
- [9] Erdogan, M. Emin, and C. Erdem Imrak. "On unsteady unidirectional flows of a second grade fluid." *International Journal of Non-Linear Mechanics* 40, no. 10 (2005): 1238-1251. <https://doi.org/10.1016/j.ijnonlinmec.2005.05.004>
- [10] Wang, C. Y. "Two-fluid oscillatory flow in a channel." *Theoretical and Applied Mechanics Letters* 1, no. 3 (2011): 032007. <https://doi.org/10.1063/2.1103207>
- [11] Wang, Chang Yi. "Starting flow in a rotating parallel plate channel." *Acta Mechanica Sinica* 28 (2012): 1271-1276. <https://doi.org/10.1007/s10409-012-0096-5>
- [12] Khan, M., Ehnber Naheed, C. Fetecau, and T. Hayat. "Exact solutions of starting flows for second grade fluid in a porous medium." *International Journal of Non-Linear Mechanics* 43, no. 9 (2008): 868-879. <https://doi.org/10.1016/j.ijnonlinmec.2008.06.002>
- [13] Hayat, Tasawar, Naveed Ahmed, M. Sajid, and Saleem Asghar. "On the MHD flow of a second grade fluid in a porous channel." *Computers & Mathematics with Applications* 54, no. 3 (2007): 407-414. <https://doi.org/10.1016/j.camwa.2006.12.036>
- [14] Sharma, Bhupesh Dutt, Pramod Kumar Yadav, and Anatoly Filippov. "A Jeffrey-fluid model of blood flow in tubes with stenosis." *Colloid Journal* 79 (2017): 849-856. <https://doi.org/10.1134/S1061933X1706014X>
- [15] Ewis, Karem Mahmoud. "Analytical solution of modified Bingham fluid flow through parallel plates channel subjected to Forchheimer medium and Hall current using linearized differential transformation method." *Journal of Advanced Research in Numerical Heat Transfer* 4, no. 1 (2021): 14-31.
- [16] Ewis, Karem Mahmoud. "Effects of Variable Thermal Conductivity and Grashof Number on Non-Darcian Natural Convection Flow of Viscoelastic Fluids with Non Linear Radiation and Dissipations." *Journal of Advanced Research in Applied Sciences and Engineering Technology* 22, no. 1 (2021): 69-80. <https://doi.org/10.37934/araset.22.1.6980>
- [17] Sharma, Bhupesh Dutt, and Pramod Kumar Yadav. "A mathematical model of blood flow in narrow blood vessels in presence of magnetic field." *National Academy Science Letters* 42 (2019): 239-243. <https://doi.org/10.1007/s40009-018-0718-y>
- [18] Khanukaeva, D. Yu, A. N. Filippov, P. K. Yadav, and A. Tiwari. "Creeping flow of micropolar fluid through a swarm of cylindrical cells with porous layer (membrane)." *Journal of Molecular Liquids* 294 (2019): 111558. <https://doi.org/10.1016/j.molliq.2019.111558>
- [19] Yadav, Pramod Kumar. "Slow motion of a porous cylindrical shell in a concentric cylindrical cavity." *Meccanica* 48 (2013): 1607-1622. <https://doi.org/10.1007/s11012-012-9689-0>
- [20] Yadegari, Mehrdad, and Mahdi Jahangiri. "Simulation of non-uniform magnetic field impact on nonNewtonian and pulsatile blood flow." *Journal of Advanced Research in Fluid Mechanics and Thermal Sciences* 57, no. 1 (2019): 86-99.
- [21] Ansari, Iftekhar Ahamad, and Satya Deo. "Effect of magnetic field on the two immiscible viscous fluids flow in a channel filled with porous medium." *National Academy Science Letters* 40 (2017): 211-214. <https://doi.org/10.1007/s40009-017-0551-8>
- [22] Srinivas, Suripeddi, Challa Kalyan Kumar, and Anala Subramanyam Reddy. "Pulsating flow of Casson fluid in a porous channel with thermal radiation, chemical reaction and applied magnetic field." *Nonlinear Analysis: Modelling and Control* 23, no. 2 (2018): 213-233. <https://doi.org/10.15388/NA.2018.2.5>
- [23] Bhat, Ashwini, Param Tangsali, and Nagaraj Nagesh Katagi. "Application of Keller-Box Method to the Heat and Mass Transfer Analysis of Magnetohydrodynamic Flow of Micropolar Fluid between Porous Parallel Walls of Different

- Permeability." *Journal of Advanced Research in Fluid Mechanics and Thermal Sciences* 102, no. 2 (2023): 186-195. <https://doi.org/10.37934/arfmts.102.2.186195>
- [24] Devi, M. Padma, and S. Srinivas. "Two layered immiscible flow of viscoelastic liquid in a vertical porous channel with Hall current, thermal radiation and chemical reaction." *International Communications in Heat and Mass Transfer* 142 (2023): 106612. <https://doi.org/10.1016/j.icheatmasstransfer.2023.106612>
- [25] Mahmoudi, Yasser. "Constant wall heat flux boundary condition in micro-channels filled with a porous medium with internal heat generation under local thermal non-equilibrium condition." *International Journal of Heat and Mass Transfer* 85 (2015): 524-542. <https://doi.org/10.1016/j.ijheatmasstransfer.2015.01.134>
- [26] Yang, Kun, and Kambiz Vafai. "Analysis of temperature gradient bifurcation in porous media—an exact solution." *International Journal of Heat and Mass Transfer* 53, no. 19-20 (2010): 4316-4325. <https://doi.org/10.1016/j.ijheatmasstransfer.2010.05.060>
- [27] Boutin, Claude, Jean-Louis Auriault, and Christian Geindreau. *Homogenization of coupled phenomena in heterogenous media*. Vol. 149. John Wiley & Sons, 2010.
- [28] Umavathi, J. C., Ali J. Chamkha, Abdul Mateen, and A. Al-Mudhaf. "Unsteady oscillatory flow and heat transfer in a horizontal composite porous medium channel." *Nonlinear analysis: Modelling and control* 14, no. 3 (2009): 397-415. <https://doi.org/10.15388/NA.2009.14.3.14503>
- [29] Ananth, S. P. V., B. N. Hanumagowda, S. V. K. Varma, C. S. K. Raju, I. Khan, and P. Rana. "Thermo-diffusion impact on immiscible flow characteristics of convectively heated vertical two-layered Baffle saturated porous channels in a suspension of nanoparticles: an analytical study." *Applied Mathematics and Mechanics* 44, no. 2 (2023): 307-324. <https://doi.org/10.1007/s10483-023-2956-6>